

## Preface

W. P. Kustas

Hydrology Laboratory, Agricultural Research Service, U.S. Department of Agriculture, Beltsville, Maryland

D. C. Goodrich

Southwest Watershed Research Center, Agricultural Research Service, U.S. Department of Agriculture  
Tucson, Arizona

**Abstract.** The Monsoon '90 multidisciplinary field campaign was conducted over the U.S. Department of Agriculture's Agricultural Research Service Walnut Gulch experimental watershed in southeastern Arizona during June–September 1990. A primary objective of this combined ground, aircraft, and satellite campaign was to assess the feasibility of utilizing remotely sensed data coupled with water and energy balance modeling for large-area estimates of fluxes in semiarid rangelands. The experimental period encompassed a variety of vegetation, soil moisture, and rainfall conditions characterized by large temporal and spatial gradients. This preface outlines experimental objectives, briefly discusses the field campaigns, summarizes initial observations, and provides an overview of articles that are a part of the Monsoon '90 special section.

## Introduction

Accurate characterization and quantification of the components of the hydrologic cycle and surface energy balance over a wide range of scales must be accomplished to advance our understanding and ability to model land surface and climatic interactions [National Research Council, 1991]. Observations have shown that land surface anomalies, in which water and energy fluxes significantly deviate from the surrounding region, influence local and regional climate [Stidd, 1975; Segal *et al.*, 1989]. Therefore it is imperative that climate models contain an interactive surface hydrology component in order to properly link land surface fluxes and atmospheric processes [Eagleson, 1986].

This is a difficult task in any region, but the challenge is compounded in arid and semiarid regions due to the relative extremes and large spatial and temporal gradients encountered in water and energy balance components. With roughly one third of the Earth's landmass considered arid or semiarid rangeland [Branson *et al.*, 1972], it is imperative that we attempt to better understand the reciprocal relationship between the hydrologic cycle and local and regional climate. In addition, semiarid rangelands contain ecosystems that are sensitive to climate anomalies and anthropogenic effects. Because of the strong correlation between ecosystem changes and changes in the water and surface energy balance [Schlesinger *et al.*, 1990], it is important to be able to monitor these changes at synoptic scales.

Synoptic understanding of the water and energy balance and monitoring of the many associated variables will require large-scale interdisciplinary field campaigns which combine integrated traditional ground and atmospheric measurements with remotely sensed measurements made at a variety of scales. The Hydrologic Atmospheric Pilot Experiment and Modélisation du Bilan Hydrique (HAPEX-MOBILHY) [An-

This paper is not subject to U.S. copyright. Published in 1994 by the American Geophysical Union.

Paper number 93WR03068.

dré *et al.*, 1986], the First International Satellite Land Surface Climatology Project (ISLSCP) Field Experiment (FIFE) [Sellers *et al.*, 1988], and the semiarid Botswana savanna experiment [van de Griend *et al.*, 1989] exemplify this approach. The purpose of Monsoon '90 was to employ a parallel multidisciplinary campaign approach to explore the utility of coupling remotely sensed and traditional measurements with energy and water balance models for large-area estimates of the fluxes in semiarid rangelands.

Specific objectives of the project are as follows [Kustas *et al.*, 1991]:

1. Integrate remote sensing observations over a wide range of pixel resolutions from ground-, aircraft- and satellite-based systems in order to assess the effects of a complex surface on sensor integration.
2. Investigate the utility of remote sensing at various wavelengths for mapping the spatial distribution of geophysical variables such as soil moisture, surface temperature, and vegetation biomass.
3. Quantify basin-scale energy fluxes with models that utilize atmospheric boundary layer data and evaluate their sensitivity to local precipitation events which result in spatial variation in soil moisture.
4. Evaluate the use of remote sensing information as input into a rainfall-runoff model for determining the hydrologic response of a semiarid basin to a precipitation event.
5. Develop and test models which can utilize remote sensing of key input variables for evaluating the exchange of water vapor and energy across the soil-plant-atmospheric interface.

## Location of Study Site

The study area was located within the Walnut Gulch experimental watershed (31°43'N 110°W) operated by the U.S. Department of Agriculture's Agricultural Research Service (USDA ARS) Southwest Watershed Research Center. Formal research and data collection was initiated on the

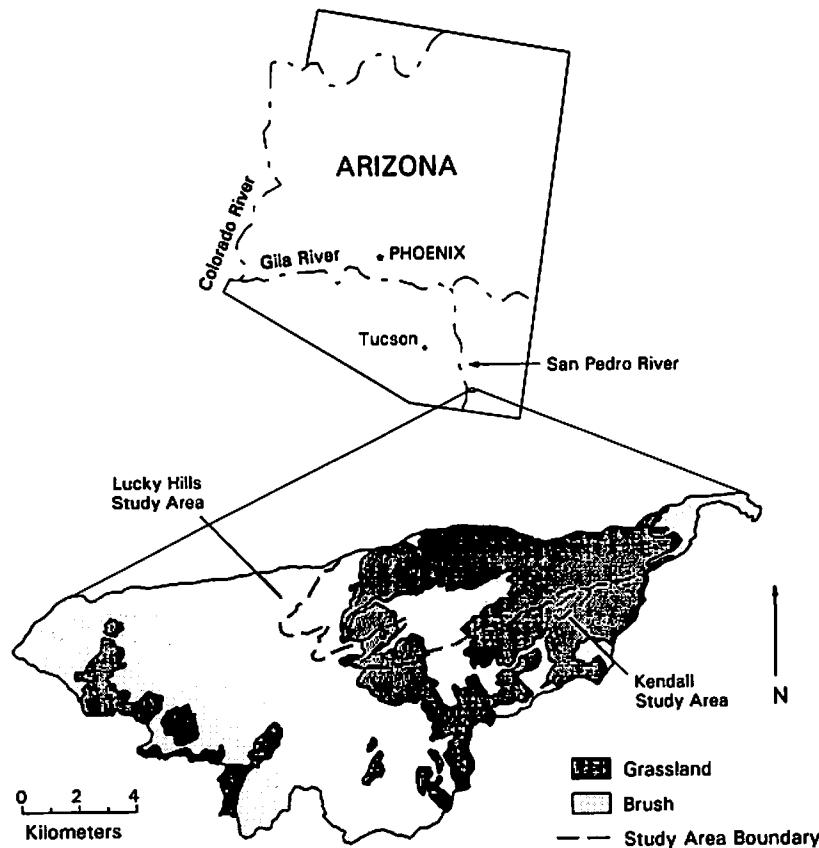


**Figure 1.** Schematic illustrating location and boundaries of the USDA ARS Walnut Gulch experimental watershed in Arizona. Areas defined as either a grass- or shrub-dominated ecosystem are mapped, and the boundary of the main study area along with the location of the two main experimental subwatersheds, Lucky Hills and Kendall, is given.

watershed in 1954. The resulting knowledge base and database [Renard, 1970; Renard *et al.*, 1993] made Walnut Gulch an ideal location to address the Monsoon '90 research objectives. The catchment is an ephemeral tributary of the San Pedro River, with the instrumented area composing the upper 150 km<sup>2</sup> of the Walnut Gulch drainage basin (see Figure 1). A false color image from an April 1982 Landsat 3 multispectral scanner (MSS) scene in Plate 1 provides a synoptic view of the San Pedro Basin and shows the size and location of the Walnut Gulch watershed relative to the surrounding region. The areas with more intense red tones indicate an increase in vegetation cover. These areas are mainly located along the rivers and tributaries, in higher elevations (mountain ranges) and in regions with irrigation (agricultural farms). The exploded view of the watershed in Plate 1 is from the September 9, 1990, Landsat 5 thematic mapper (TM) scene. The image illustrates in much greater detail the drainage patterns, topographic features, and areas with higher vegetation cover.

The annual precipitation varies from 250 to 500 mm with approximately two thirds falling during the "monsoon" season (July–September). The surface soil (0–5 cm) textures are gravelly loamy sands and sandy loams, and the soils typically contain a small quantity of organic matter. The rock content for the 0–5 cm layer averaged around 30%, while the surface rock fraction was of the order of 50%. This high rock content in the near-surface soils complicates measurements of soil moisture and heat fluxes, the modeling

of the soil hydrologic and thermal properties, and the interpretation of the remotely sensed data. The vegetation is a mixed grass-brush rangeland typical for southeastern Arizona and southwestern New Mexico. The western half of the watershed is brush dominated, while the eastern half contains primarily grasses. Vegetation cover ranges from ~20% to ~60%. Also in Figure 1 the approximate boundaries of the main vegetation biomes in the watershed and outlines of the main study area are illustrated. The watershed has hilly topography with steep incised ephemeral channels in alluvium from the nearby Driest Mountains. The main drainage runs from the northeast to the southwest (~220° from north) with the main outlet at the west end of the watershed. The elevation changes from about 1800 m above mean sea level (MSL) at the northeast corner of the basin to 1300 m MSL roughly 25 km west at the outlet. The topography becomes more dissected toward the eastern end of the study area. Typical ridge to valley heights are of order 10 m at the western end and increase to 15–20 m in the eastern half of the study area. Typical spacing between ridgetops is around 500 m. The high degree of dissection in the north central portion of the watershed is readily apparent in the exploded view of the watershed in Plate 1. Figure 2 illustrates the main drainage patterns in the watershed and the location of 92 rain gages and 11 large runoff-measuring stations. The stream gage network permits the basin to be subdivided into 11 subwatersheds varying in size from 2.3 km<sup>2</sup> up to 150 km<sup>2</sup>.

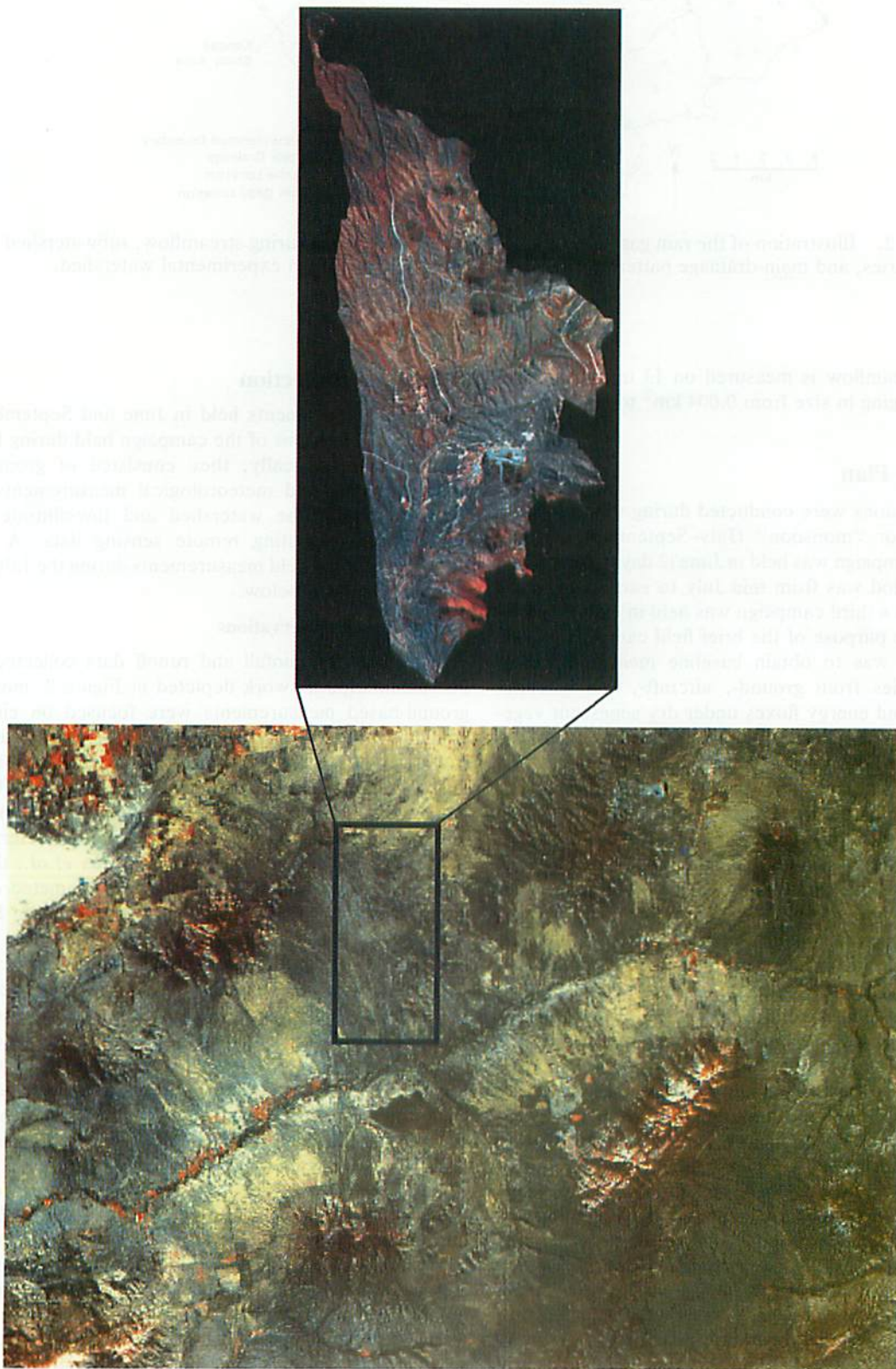


**Plate 1.** A false color image of the San Pedro Basin generated from a Landsat 3 MSS image collected in April 1982. The exploded view of the watershed was extracted from a Landsat 5 TM scene obtained on September 9, 1990. For both images, the red tones indicate more vegetation cover.

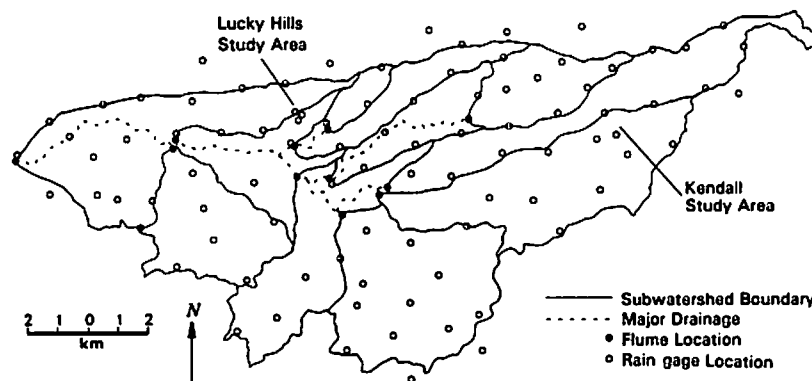


Figure 2. Illustration of the rain gage network, flume locations for measuring streamflow, subwatershed boundaries, and main drainage pattern for the USDA ARS Walnut Gulch experimental watershed.

In addition, streamflow is measured on 13 intensive small watersheds, ranging in size from 0.004 km<sup>2</sup> to 0.89 km<sup>2</sup>.

### Experimental Plan

Field observations were conducted during the dry (May–June) and wet or “monsoon” (July–September) seasons. The first field campaign was held in June (2 days), the second observation period was from mid July to early August (20 day period), and a third campaign was held in early September (1 day). The purpose of the brief field campaign during the dry season was to obtain baseline measurements of surface properties from ground-, aircraft-, and satellite-based sensors and energy fluxes under dry senescent vegetation and dry soil moisture conditions. The objective of the second campaign was to collect data when the vegetation was at its peak greenness and there was a high probability that significant precipitation events would produce runoff in the basin. Moreover, the localized nature of these precipitation events results in significant spatial and temporal variability in soil moisture conditions. This provides an interesting set of conditions to test both the utility of the remote sensing data and the capability of models to evaluate the energy and water balance over a range of spatial and temporal scales. The purpose of the third field campaign was to try to collect usable satellite data from SPOT and Landsat which were not obtainable during the July–August observation period.

The contrast in surface conditions for the study site between the dry, premonsoon, and the peak greenness conditions in the monsoon season can be seen in Plate 2, which consists of the SPOT 1 high-resolution visible sensor (HRV) 1 scene for June 5, 1990, and Landsat 5 TM scene from September 9, 1990. The digital counts were converted to apparent reflectances, and a soil-adjusted vegetation index (SAVI) [Huete, 1988] was computed for each pixel. For the June scene most SAVI values are below 0.1, except in the town of Tombstone where lawns were irrigated. For the September image the vegetation response to the monsoon rains results in SAVI values 2–3 times higher than in June. Also note that many of the drainage patterns are discernible in the September scene and that there is a tendency for higher SAVI values in the grass-dominated region.

### Field Data Collection

The field experiments held in June and September were scaled-down versions of the campaign held during the monsoon season. Basically, they consisted of ground-based remote sensing and meteorological measurements at two locations within the watershed and low-altitude aircraft observations collecting remote sensing data. A detailed description of the field measurements during the July–August campaign is given below.

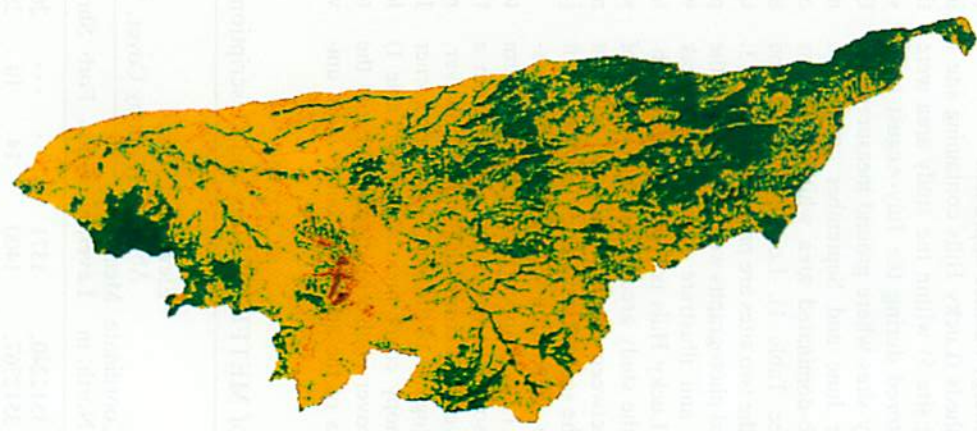
#### Ground-Based Observations

In addition to rainfall and runoff data collected by the instrumentation network depicted in Figure 2, most of the ground-based measurements were focused on eight sites which covered the main vegetation biomes in the region. At each site, there were continuous measurements of meteorological conditions at screen height, near-surface soil temperature and soil moisture, surface temperature, incoming solar and net radiation, soil heat flux, and indirect determination of sensible and latent heat fluxes [Kustas *et al.*, this issue (a)]. The approximate locations of these meteorological–energy flux (METFLUX) stations is illustrated in Figure 3. Samples of the soil and vegetation were made at each METFLUX site in order to describe the soil properties and vegetation type and estimate fractional vegetation cover [Wertz *et al.*, this issue]. In addition, daily gravimetric samples of the 0–5 cm layer were collected from each site [Schmugge *et al.*, this issue]. Table 1 provides universal transverse Mercator (UTM) coordinates and elevations for each site and general soil and vegetation information. A summary of the location, type, and frequency of the ground-based measurements is provided in Table 2.

Other instrumentation for estimating the surface energy balance was located at several of the METFLUX sites during the July–August campaign. One system measured the sensible heat flux using the eddy correlation technique with a propeller anemometer and fine wire thermocouple situated on a 9-m tower [Stannard *et al.*, this issue]. These systems were located at five of the eight stations. Fluxes of latent and sensible heat were also measured by two one-dimensional eddy correlation systems. The instruments included a sonic anemometer with a fine wire thermocouple and a krypton hygrometer at a nominal height of 2 m above the ground [Stannard *et al.*, this issue]. One of the one-dimensional



(a)



(b)



**Plate 2.** False color soil-adjusted vegetation index (SAVI) images of the Walnut Gulch watershed from the SPOT 1 HRV 1 on June 5, 1990, and from Landsat 5 TM on September 9, 1990. Rains from the “monsoon season” cause a peak in vegetation “greenness” resulting in a significant increase in SAVI values from the dry season (see text).

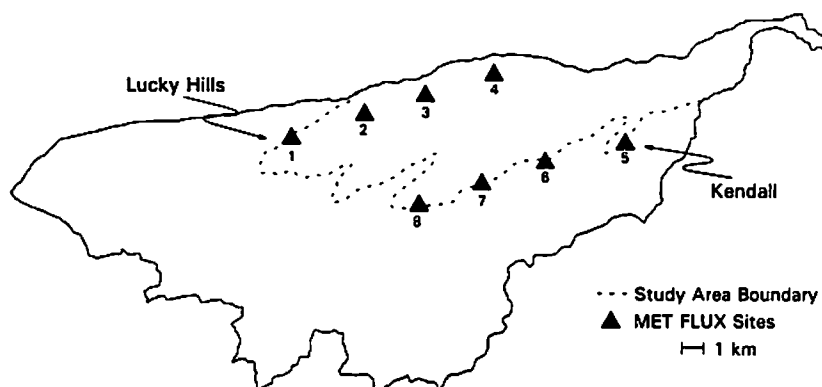


Figure 3. Location of METFLUX sites within the study area. The intensively studied subwatersheds (supersites) Lucky Hills and Kendall are labeled (see text).

systems was transported to several of the METFLUX sites. The two supersites also contained a gradient-measuring system for estimating the latent and sensible heat fluxes using the Bowen ratio energy balance approach.

Two small subwatersheds (Lucky Hills containing site 1 and Kendall containing site 5) within the study area were more intensively monitored during the July-August campaign and were the only sites where ground measurements were made during the June and September campaigns. Lucky Hills is a shrub-dominated area while Kendall is primarily grassland (see Table 1). Low-level aerial and ground photographs of the two sites are presented in Plate 3. Both of the ground-based photographs were taken during the July-August campaign and illustrate vegetation at peak greenness. The site at Lucky Hills is typical of the brush-dominated portions of the study area with a high degree of spatial heterogeneity between brush clumps and adjacent bare soil occurring on the scale of a meter or less (lower left part of Plate 3). The vegetation cover for the grass-dominated Kendall site (site 5) appears to be more uniform with nearly complete soil coverage when viewed from a ground perspective (lower right corner of Plate 3). However, the low-level aerial photograph of the site (upper right corner of Plate 3) and the canopy cover measurements (Table 1) clearly show that the cover is also relatively sparse in the grass-dominated regions of the study site but is more uni-

formly distributed than the brush site. Soil temperature and moisture were measured at multiple depths from about 5 to 50 cm using thermocouple and time domain reflectometry (TDR) probes. At Lucky Hills the measurements were made in open areas and underneath vegetation, while at Kendall the measurements were made on north and south facing slopes midway between the stream channel and the ridge. Ground-based remote sensing observations in the visible, near-infrared and thermal-infrared wave bands were made over designated areas at Kendall and Lucky Hills during aircraft and satellite remote sensing missions [Moran *et al.*, this issue (b)]. These measurements represented multiple pixels observed from airborne and satellite sensors. There was also continuous monitoring of the soil and vegetation temperatures using mounted infrared thermometers at the supersites. At Kendall, bidirectional reflectance measurements were made with a high-resolution spectral radiometer [Qi *et al.*, this issue].

Other ground-based observations included sky view photographs taken at half-hourly intervals for assessing fractional cloud cover and type [see Pinker *et al.*, this issue] and measurements of optical depth on days with SPOT and Landsat overpasses. Both tethered and free soundings of the lower atmosphere provided profiles of dry and wet bulb temperatures, pressure, wind speed, and direction. There were two tethered systems which provided measurements

Table 1. Location of METFULX Sites and Description of Vegetation Cover and Surface Soil Properties

METFLUX Site	UTM* East, m	Coordinate North, m	Elevation Above Mean Sea Level, m	Canopy Cover, %			Soil Composition (0-5 cm), %			Surface Rock Cover, %	Rock Content (0-5 cm), %	Bulk Density, g/cm <sup>3</sup>	Organic Matter, %
				Grass	Forb	Shrub	Sand	Slit	Clay				
1	589843.	3512240.	1371	...	...	26	66	24	10	46	28	1.64	0.81
2	592251.	3512767.	1400	14	10	28	69	20	11	48	36	1.83	NA
3	594945.	3513344.	1452	5	3	38	71	20	9	45	28	1.58	0.58
4	596862.	3513748.	1492	42	6	13	73	22	5	59	45	1.82	0.88
5	600288.	3511499.	1526	35	1	4	69	20	11	54	38	1.61	1.75
6	596104.	3510611.	1460	5	4	28	67	25	8	52	31	1.44	1.67
7	593439.	3510040.	1393	14	6	12	80	14	6	10	10	1.74	0.52
8	591091.	3509527.	1375	...	1	38	72	20	8	58	21	1.47	0.72

NA denotes not available.

\*Zone 12, NAD 1927.

**Table 2. Location, Height/Depth, and Frequency of Ground-Based Hydrometeorological and Remote Sensing Observations**

Measurement Type	Sites	Nominal Height (Depth), m	Frequency
Air temperature	1-8	4	continuous
Air temperature	1, 5-8	9	continuous
Temperature/relative humidity	1, 5	2	continuous
Wind speed and direction	1-8	4.5	continuous
Solar radiation	1-8	3.5	continuous
Net radiation/surface temperature	1-8	3	continuous
Photosynthetically active radiation	1, 5	3.5	continuous
Soil heat flux	1-8	(0.05)	continuous
Soil temperature	1-8	(0.025), (0.05), (0.15)	continuous
Soil moisture (resistance sensors)	1-8	(0.025), (0.05)	continuous
Soil moisture (TDR)	1, 5	(0.05)-(0.50)	daily
Soil moisture (gravimetric)	1-8	(0-0.05)	daily
Rainfall	85*	1	continuous
Runoff	23†	...	continuous
Remote sensing	1, 5	1	satellite, aircraft‡
Free radio soundings	1§	0-4000	periodic
Tethered soundings	1, 5	0-500	periodic

Data request inquiries can be directed to Jane Thurman, USDA ARS, Water Data Center, Hydrology Laboratory, Building 007, Room 104, BARC-West, Beltsville, MD 20705 (phone 301-504-9411). Phone modem access for database overview and downloading can be obtained at the following number: 301-504-8154 (Hayes compatible, 8 bits per word, 1 stop bit, no parity, local echo off, 300/1200/2400 BPS).

\*There are 85 weighing rain gages for the entire Walnut Gulch watershed at the time of the experiment (150 km<sup>2</sup>).

†There are 11 primary runoff measuring stations for the large subwatersheds (2.3-150 km<sup>2</sup>) and 13 stations for small research watersheds (0.4-89 ha), excluding monitored ponds.

‡Ground-based observations taken during aircraft and Landsat and SPOT overpasses (see Table 3 for more details).

§Free soundings were also taken at several other locations within and near the Walnut Gulch watershed.

up to about 500 m above ground level (AGL), while the free soundings provided profiles up to around 4000 m AGL. The two tethered systems were separated by about 10 km along a line parallel to the general wind directions in the lower atmosphere for investigating advection effects [Hippis *et al.*, this issue].

#### Aircraft Observations

Three aircraft were used on a regular basis during the July-August campaign. A Cessna aircraft flown by Aerial Images Corporation, Tucson, Arizona, carried multispectral radiometers, an infrared thermometer, and a thermal-infrared scanner. (Product and company names are given for the benefit of the reader and imply no endorsement by USDA.) An Aero Commander from the USDA ARS Subtropical Agricultural Research Lab in Weslaco, Texas, flew a three-band microwave radiometer and a laser profiling system. The NASA C-130 aircraft, based out of Ames Research Center, California, carried multifrequency radiometers covering the visible, near-infrared, and thermal-infrared wavebands. It also had a microwave radiometer on board and large format mapping cameras. All three aircraft contained video systems for georeferencing the data. A fourth aircraft, NASA DC-8 from Ames Research Center, flew the synthetic aperture radar (SAR) over the watershed in early spring and once during the July-August campaign. Table 3 gives a general description of the instruments flown on each aircraft and flight dates.

The Cessna and Aero Commander missions usually consisted of flying three transects at an altitude between 100 and 150 m AGL. Two of the transects were parallel, running

roughly east-west and covered the METFLUX stations. The third flight line ran northwest-southeast traversing the other two flight paths. Figure 4a illustrates the location of the flight lines on the watershed. The pixel sizes from the sensors on the Cessna were around 25 m, except for the thermal scanner data which were of the order of 0.20 m. The three-band microwave radiometer on the Aero Commander gave a pixel size of order 100 m, while the laser produced a pixel size around 0.05 m. This microwave radiometer was successfully used to sense soil moisture, and results derived from it are reported by Jackson *et al.* [1992].

The C-130 flew two distinct missions depending upon the instruments being used. A low-altitude mission (~600 m AGL) collected data from the push broom microwave radiometer (PBMR) and NS001 instruments while a midaltitude (~2000 m AGL) and high-altitude mission (~5000 m AGL) used the thermal imaging multispectral scanner (TIMS) and NS001 sensors. The flight lines for the low-altitude, midaltitude, and high-altitude missions are shown in Figure 4. The pixel size for the PBMR flights was around 180 m, while the NS001 had pixel sizes of 1.5 m, 6 m, 12.5 m, for the low-altitude, midaltitude, and high-altitude missions. The TIMS produced similar pixel-sized footprints as the NS001 for the midaltitude and high-altitude flights. For the SAR the flying altitude was over 7500 m AGL, yielding a sensor resolution of order 10 m. The DC-8 overpasses were somewhere between line 1 and line 2 in Figure 4c.

#### Satellite Observations

An attempt was made to collect satellite data from SPOT 1, SPOT 2, Landsat 5, NOAA 11 advanced very high

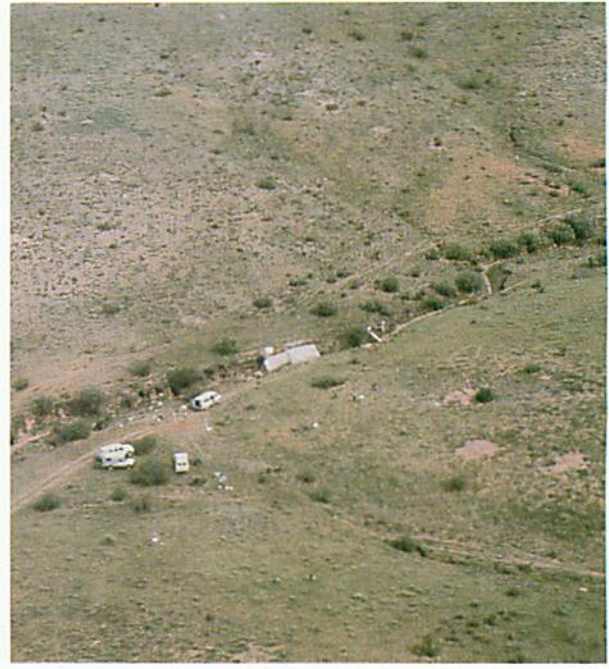


**Plate 3.** A collection of photographs representative of the shrub- and grass-dominated ecosystems of the region. (top left) Low-level aerial photograph looking northeast at METFLUX site 1 (Lucky Hills, brush-dominated). (bottom left) Ground cover photograph looking northwest of site 1. (top right) Low-level aerial photograph looking north at METFLUX site 5 (Kendall, grass-dominated). (bottom right) Ground cover photograph looking northeast of site 5.

resolution radiometer (AVHRR), and GOES 7 for all three field campaigns. Table 4 lists some general sensor information for the satellites employed in this study and acquisition dates. The higher than normal frequency of cloud cover during the July-August campaign resulted in a smaller number of usable scenes than what was expected. In fact, due to the low temporal frequency of coverage of the watershed by SPOT 2 and Landsat 5, no satisfactory images were available for the July-August campaign. However, these satellites did provide usable images for the June and September field campaigns [Moran *et al.*, this issue (a)]. There were an adequate number of usable images of the region collected by

GOES 7 to investigate the utility of satellite remote sensing information for radiation modeling at the basin scale [Pinker *et al.*, this issue].

#### Remote Sensing Data and Scaling Issues

In Plate 4, two false color images are displayed from the thermal scanner observations collected on the Cessna aircraft. The data are from day of year (DOY) 209 at 1021 mountain standard time (MST) and at 1439 MST over METFLUX site 6 (see Figure 3). The pixel size in these images is roughly 16.5 cm, and the black circle represents the approximate area (about 30 m in diameter) integrated by

**Table 3.** General Description of Instruments Flown on the Cessna, Aero Commander, and C-130 Aircraft and Flight Dates

Aircraft	Instrument	Number of Bands	Wavelength Range	Aircraft Flight Dates, day of year
Cessna	Exotech radiometer; IFOV, 15°	4	0.50–0.89 $\mu\text{m}$ (SPOT filters) 0.45–0.90 $\mu\text{m}$ (TM filters)	156, 204, 209, 211, 212, 214, 216, 217, 220, 221, 222
Cessna	Everest infrared thermometer; IFOV, 15°	1	8–13 $\mu\text{m}$	156, 204, 209, 211, 212, 214, 216, 217, 220, 221, 222
Cessna	multispectral video camera; IFOV, 15°	6	0.48–0.90 $\mu\text{m}$	156, 204, 209, 211, 212, 214, 216, 217, 220, 221, 222
Cessna	thermal infrared scanner; IFOV, 2.4 mrad	1	8–12 $\mu\text{m}$	156, 204, 209, 211, 212, 214, 216, 217, 220, 221, 222
Aero Commander	multifrequency microwave radiometer	3	2.25–27 cm	211, 212, 214, 215, 216, 217, 218, 221
Aero Commander	pulsed gallium-arsenide diode laser profiler; IFOV, 1 mrad	1	0.904 $\mu\text{m}$	see footnote
C-130	NS001 thematic mapper simulator; IFOV, 2.5 mrad; scan angle, 100°	8	0.458–12.3 $\mu\text{m}$	212, 213, 214, 216, 217, 220, 221, 222
C-130	thermal imaging multispectral scanner (TIMS); IFOV, 2.5 mrad; scan angle, 76°	6	8.2–11.7 $\mu\text{m}$	212, 213, 214, 216, 217, 220, 221, 222
C-130	push broom microwave radiometer (PBMR); IFOV, 17°; FOV, 50°	1	21 cm	212, 214, 216, 217, 220, 221

IFOV denotes instantaneous field of view. Due to instrument malfunction in 1990, laser profiler data were acquired over the same locations and under similar conditions in 1991.

the thermal-infrared radiometer on board the aircraft (Table 3). The heterogeneity of surface cover and brightness temperature is readily apparent. The cooler areas in light purple are the large clumplike brush species commonly known as beargrass (*Nolina microcarpa* Wats.) The variation in brightness temperature evident in the images and indicated by the accompanying histograms suggests differences between the beargrass and the adjacent bare ground ranged from 10°C to 15°C. This large brightness temperature variation on a sub-meter scale caused by sparse, mixed vegetation canopies poses significant challenges when interpreting larger pixel imagery (commonly of the order of 10<sup>1</sup> to 10<sup>3</sup> m) and in the modeling of the surface energy balance at various length scales.

The effect of sensor resolution on the observed spatial variation in brightness temperature for the study area is

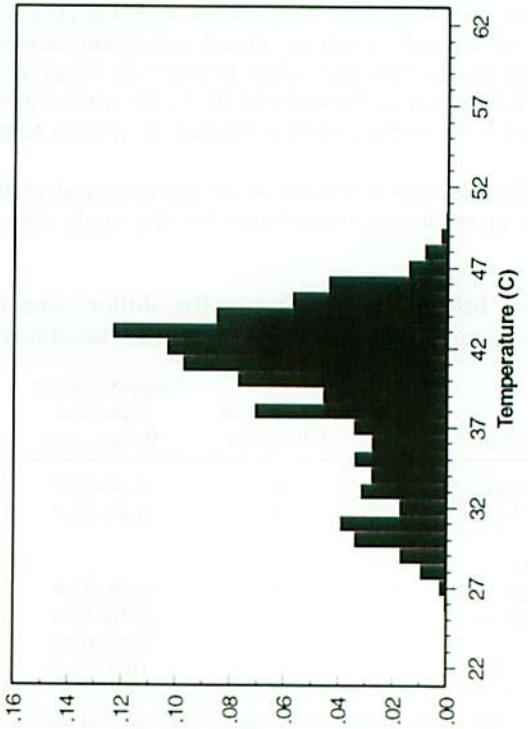
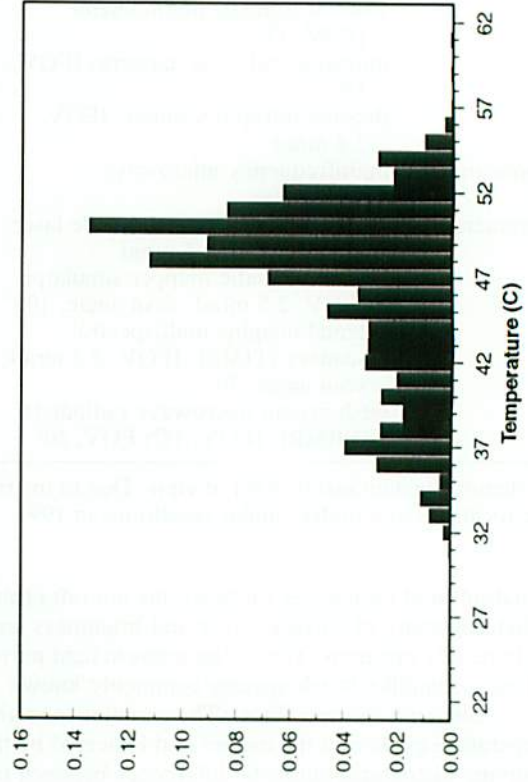
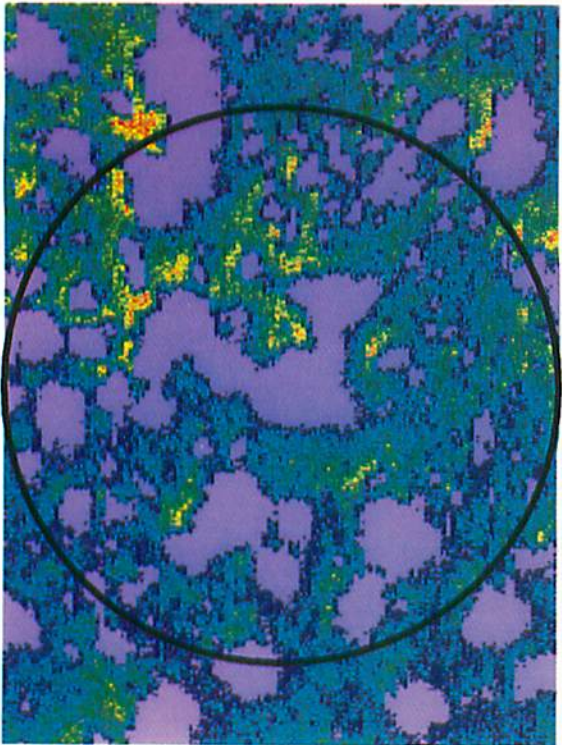
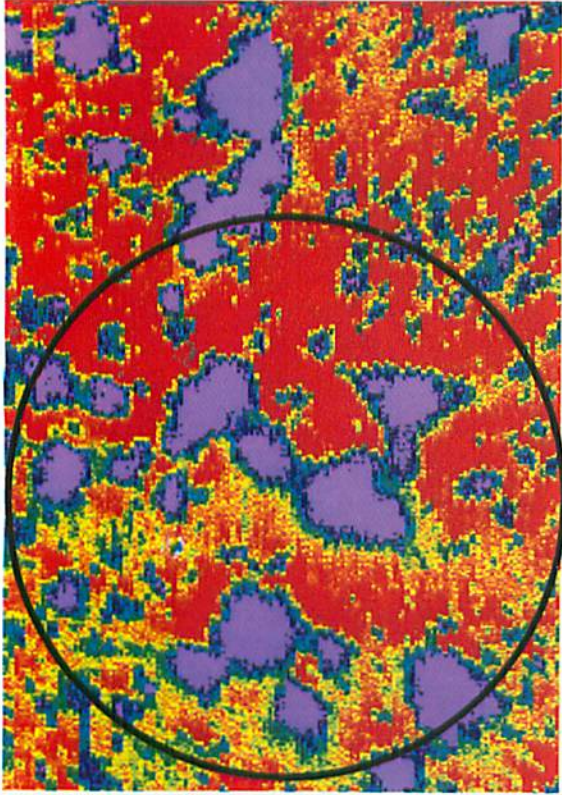
illustrated in Plate 5 with a sequence of images from the NS001 instrument flown on the C-130 (Table 3). The image is from DOY 216. The pixel resolution is degraded from the original 6-m pixel to 120 m and 1100 m in order to simulate the observations from Landsat TM and NOAA AVHRR satellites (Table 4). The images reveal a decrease in the spatial variability in brightness temperature and a reduced sensitivity to topography with the coarser-resolution scenes, especially at the 1100 m pixel size. The standard deviation in average temperature for the scene decreases from nearly 20°C for the 6-m pixel to roughly 10° for the 120-m pixel to about 7°C for the 1100-m pixel. However, the difference in the average temperature of the scene at the three resolutions is less than 0.5°C. Furthermore, notice that even with a significant degradation in resolution, the overall pattern in brightness temperature values for the scene is still present.

**Table 4.** Information on Sensor Resolution, Spectral Range, Number of Channels, and Temporal Frequency and Acquisition Dates for the Satellite Platforms Used in This Study

Satellite	Number of Channels	Approximate Spectral Range, $\mu\text{m}$	Pixel Resolution	Temporal Frequency	Acquisition Dates, day of year
SPOT 1 and 2 (HRV)	4	0.50–0.89	20 m	5 days	156, 252
Landsat 5 (TM)	7	0.45–12.5	30 m visible and IR 120 m thermal-IR	18 days	156, 252
NOAA 11					
AVHRR-LAC	5	0.58–12.5	1.1 km	12 hours	156, 208, 209, 216, 221
AVHRR-GAC	5	0.58–12.5	4.5 km		
GOES 7	2	0.55–0.75 10.5–12.5	8 km	...*	156, 207–222

LAC denotes local area coverage; GAC, global area coverage.

\*Eleven visible and five infrared observations over a 24-hour period.



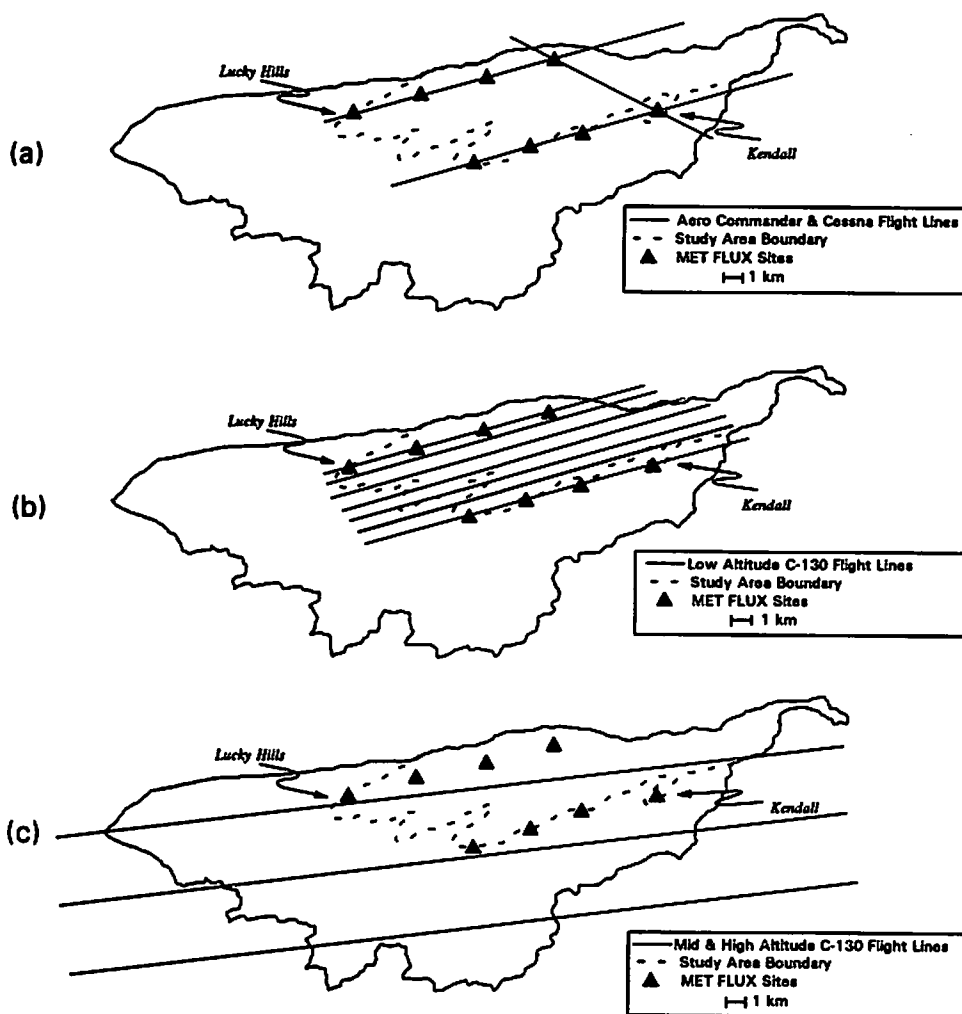


Figure 4. Flight lines for (a) the Cessna and Aero Commander low-altitude missions, (b) the low-altitude C-130 PBMR flights, and (c) the midaltitude and high-altitude C-130 TIMS/NS001 missions.

Future investigations with these data will include assessing the impact of sensor resolution and brightness temperature variability on computed fluxes.

### An Overview of the Monsoon '90 Articles

The papers can be grouped under three general topics. The first topic concerns the investigation of spatial and temporal variability of ground-truth data caused by environmental factors and measurement errors. Included are papers dealing with the correction and interpretation of the remotely sensed data. The second topic includes those papers which investigate the potential for inferring geophysical and biophysical

properties of the surface via remote sensing information. Finally, the third topic involves studies that incorporate remote sensing data and other technologies in an attempt to model the hydrologic and surface energy fluxes over a range of spatial and temporal scales.

Under the first topic, *Stannard et al.* [this issue] compared components of the surface energy balance estimated using a gradient-measuring system and eddy correlation techniques. The gradient-measuring system sampled at 1 and 2 m above the surface, while eddy correlation sensors were mounted on 2- and 9-m towers. At a site, comparison of net radiation ( $R_n$ ) measurements using the same instrument design produced relatively small differences; however, three brands of net radiation sensors produced differences greater than 10%. The soil heat flux ( $G$ ) measured by the different systems showed significant variability which was attributed mainly to measurement errors and differences in technique used in estimating the heat storage in the top 5 cm. Comparison of sensible ( $H$ ) and latent ( $LE$ ) heat fluxes among the flux systems indicated that lower values of the Bowen ratio ( $H/LE$ ) were obtained from the 9-m tower compared to the 2-m eddy correlation tower and the gradient-measuring system. This dependence on sensor height was supported qualitatively by the results from a one-dimensional diffusion-

Plate 4. (opposite) False color images from the thermal scanner instrument on board the Cessna aircraft. The images were collected on DOY 209 at (a) 1021 MST and (b) 1439 MST over METFLUX site 6. The black circle (approximately 30 m in diameter) represents the nominal resolution of the thermal infrared radiometer on board the aircraft (Table 3). The histograms show the temperature distribution observed by the thermal scanner inside the circle. The color scale indicates that areas in light purple are the coolest, which corresponds to the vegetation (see text).

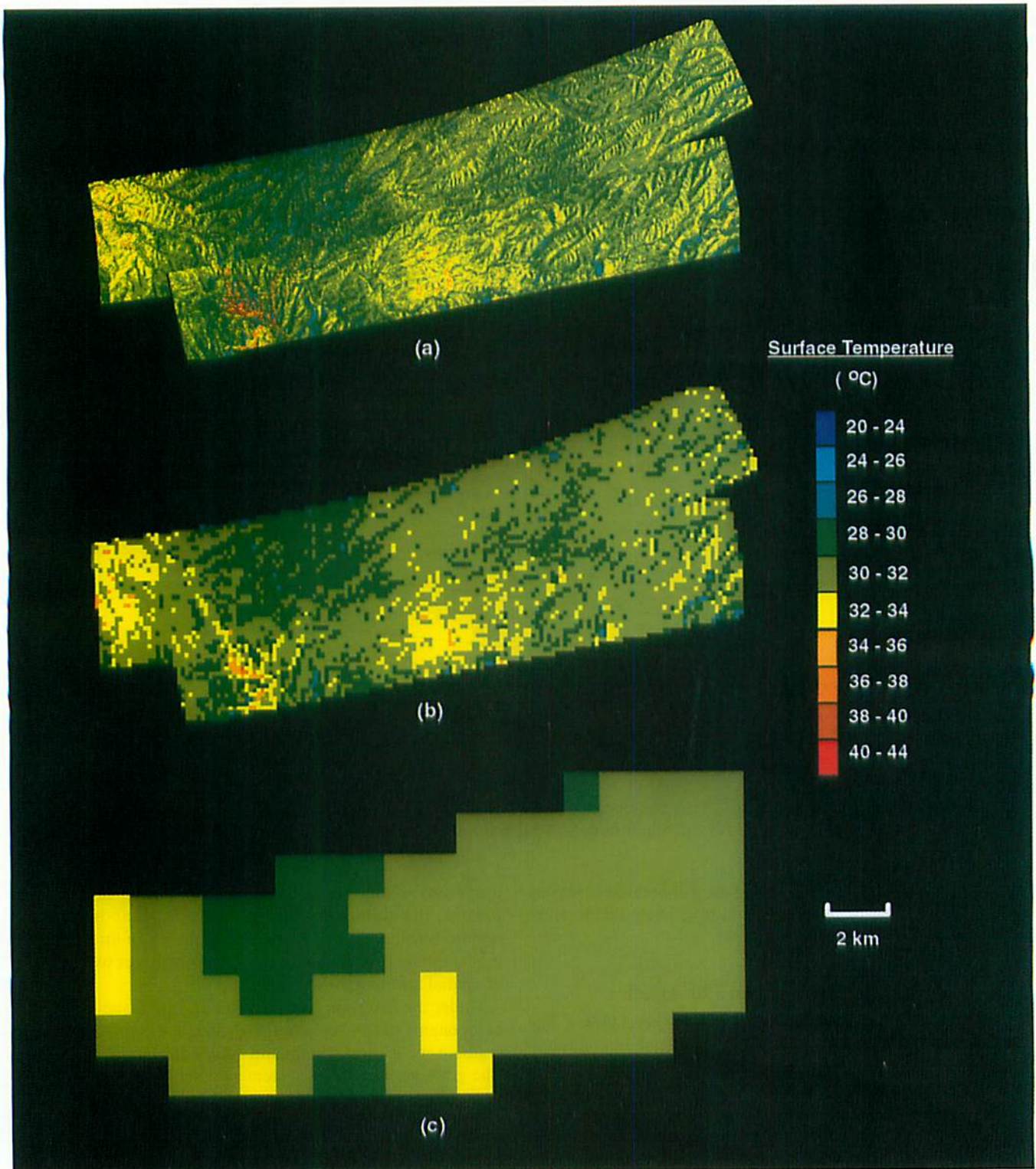


**Plate 5.** Brightness temperature images from the NS001 sensor flown on the C-130 (Table 3): (a) original 6-m pixel resolution; (b) pixel resolution degraded to 120 m, representing the Landsat TM pixels; (c) pixel resolution degraded to 1100 m, representing nadir NOAA AVHRR pixels. The overall pattern in brightness temperature values across the watershed is maintained with decreasing resolution (see text).

area model. The model indicated that the measurements from the 2-m eddy correlation tower and gradient-measuring system were more heavily weighted toward the drier and less vegetated ridgetop conditions, whereas the eddy correlation

measurements at 9 m were sampling the more vegetated ephemeral channels as well as the ridges. *Kustas et al.* [this issue (a)] computed the latent heat fluxes by having estimates of three of the four energy balance components (the

residual approach), namely  $R_n$ ,  $G$ , and  $H$ . The  $H$  values were determined indirectly by the variance method. Comparison between the 2-m eddy correlation measurements of  $H$  and  $LE$  at two sites with good fetch showed that agreement between the two techniques was within 20% for daytime conditions. Given the differences in sensor heights and approaches, the estimates of  $H$  and  $LE$  with this indirect approach were considered satisfactory and were used in several other studies in this issue.

Under the topic of interpreting remote sensing observations, *Perry and Moran* [this issue] document the potential errors in atmospheric correction of optical remote sensing data. Atmospheric data utilized by a radiative transfer model showed no correlation between radiosonde location or time and resulting temperature corrections. The corrected surface temperatures from aircraft and satellite altitudes suggest that errors in excess of 2°C can still be expected.

In another study by *Qi et al.* [this issue], bidirectional reflectance distributions measured over grassland and desert shrubs showed significant dependence on view and solar angles. This significantly affected standard vegetation indices like NDVI (normalized difference vegetation index). Yet, several candidate vegetation indices suggested by the authors demonstrated great potential for minimizing view angle effects. The impacts of view and solar zenith angles on bidirectional reflectance were also found to be vegetation cover and species dependent.

In a similar vein, *Chehbouni et al.* [this issue] utilized ground-based multiple view direction/angle measurements to validate a semiempirical model that normalizes the modified soil-adjusted vegetation index (MSAVI) computed from any view angle to nadir. In addition, a shadow parameterization was introduced into the model to simultaneously account for both Sun and view angle variations. Comparison with the observations suggested that the model provides the capability of predicting nadir viewing values of MSAVI from any off-nadir values at a given solar zenith angle. This has great potential for normalizing multiple view/Sun angle observations from satellites for the purpose of long-term vegetation monitoring.

One study utilized vegetation indices (including NDVI) and obtained surface information useful in modeling the water and energy balance. *Moran et al.* [this issue (a)] found that a soil-adjusted vegetation index (SAVI) from ground-, aircraft-, and satellite-based sensors was highly correlated with temporal changes in vegetation cover and biomass. On the other hand, quantifying the spatial variability in these quantities across the watershed was less successful. They also obtained relations between measurements of surface-air temperature differences and both daily net radiation and daily evapotranspiration that were similar to ones derived for agricultural surfaces.

A detailed study of the variation in surface temperature and emissivity was conducted by *Humes et al.* [this issue (a)]. From ground observations they found that differences between vegetation and soil background temperatures were typically 10°–25°C near midday. In addition, they discovered from ground and aircraft data that spatial variability in surface temperature at local and basin scales was similar, suggesting that under certain conditions spatial variability in surface temperature may be scale independent. Estimates of emissivity of the soil and vegetation were obtained at the

METFLUX sites. The mixture of the soil and vegetation at most sites yielded an average emissivity of about 0.98.

There were also techniques employed for estimating vegetation height and cover. *Weltz et al.* [this issue] utilized an airborne laser system for measuring landscape patterns over large areas as a way to determine mean vegetation height and cover. Estimates of vegetation height and cover were obtained from laser flights covering the METFLUX sites and were compared to ground-based line-transect methods. The agreement was quite good. Furthermore, the laser data provided the ability to separate and map distinctly different plant communities.

The utility of remote sensing for mapping surface soil moisture was tested by *Schmugge et al.* [this issue] with passive microwave data collected from the push broom microwave radiometer (PBMR). The instrument was flown at low altitude, providing maps of microwave brightness temperatures over the study area. The brightness temperatures were highly correlated to ground-based surface soil moisture measurements. The brightness temperature data were converted to soil moisture values which produced surface soil moisture maps of the study area. They also discovered that changes in the microwave brightness temperatures after a rainfall were highly correlated to the amount of rain, up to a certain threshold value.

Estimates of the local- and regional-scale aerodynamic roughness for the watershed came from the laser data analyzed by *Menenti and Ritchie* [this issue]. Values for the METFLUX sites were compared to estimates obtained from techniques using micrometeorological measurements. The agreement in the local values was quite good. Preliminary calculations of regional aerodynamic roughness were also illustrated.

Most of the efforts to evaluate the surface energy balance utilized data collected in the optical wave bands. Ground-based remote sensing data collected at the Lucky Hills and Kendall supersites were combined with conventional meteorological data by *Moran et al.* [this issue (b)] to compute the energy balance components. It was found that an additional resistance term accounting for the effect of partial vegetation cover on the radiometric temperature was needed in order to obtain satisfactory agreement between modeled and measured  $H$ . In general, flux estimates from the remote sensing model were within 10–15% of the measured values. A similar approach was taken by *Kustas et al.* [this issue (b)] with low-flying aircraft observations. The remote sensing data were averaged over a range of length scales to represent pixel sizes of order  $10^2$  to  $10^4$  m. Differences between the modeled fluxes and the values from eight METFLUX sites were less than 20% and did not vary significantly with pixel size. Similar results for estimating regional-scale energy fluxes were obtained with atmospheric boundary layer data and remote sensing data averaged over the study area. In a related approach, *Humes et al.* [this issue (b)] attempted to extrapolate energy fluxes evaluated at a reference site to other locations in the watershed using only remotely sensed inputs. The analysis indicated that significant errors can result due to the assumptions of a uniform aerodynamic resistance and incoming radiation, both of which were violated when flux estimates were extrapolated to a different ecosystem and when there were partly cloudy skies.

Basin-scale estimates of the incoming solar radiation were computed by *Pinker et al.* [this issue] using GOES data with

a solar flux inference model. The model-derived values were compared to averages from the METFLUX network and several stations outside the watershed. For a clear day, differences between 5-min ground data and "instantaneous" satellite estimates were within 3%. For a partly cloudy case the agreement was not as good. Still, for daily averaged values evaluated over the study period, there was a high correlation between the remote sensing model estimates and the average from the METFLUX network regardless of the cloud cover conditions. Differences in daily means derived from the satellite and measured by the METFLUX network were within 10%, while 5-day means were within 3% of measured.

Basin-scale energy fluxes were also evaluated using atmospheric profiles of temperature, humidity, and wind speed in the lower troposphere from radiosonde data analyzed by *Hipps et al.* [this issue]. Both latent and sensible heat fluxes were determined using the conservation equations for heat and moisture integrated over the depth of the atmospheric boundary layer from a series of soundings. The results with this approach were compared to averages given by the METFLUX network. The agreement between fluxes estimated by the integrated conservation equations and the METFLUX network was satisfactory only after accounting for large-scale advection. This was especially critical for estimating *LE* because neglecting advection often resulted in the fluxes' having the wrong sign.

Finally, it is appropriate to end this overview of papers with the study by *Goodrich et al.* [this issue]. They utilized soil moisture determined by airborne passive microwave instruments, ground-based observations, and a simple water balance model to define prestorm initial soil water content for a distributed, physically based, rainfall-runoff model. For a small and medium-sized catchment it appeared that a basin-wide average initial soil water content was sufficient for runoff simulations. This result suggests that satellite-based microwave systems which suffer from low resolution may still provide acceptable prestorm soil moisture data for computing runoff in this environment. On the other hand, this study also showed that detailed information of the rainfall distribution is critical for accurate runoff simulation.

## Concluding Remarks

Preliminary research results and data summaries from the Monsoon '90 interdisciplinary field experiment have been documented in this special section. The combination of favorable meteorological conditions and the well-instrumented ARS Walnut Gulch experimental watershed resulted in a very successful experimental campaign. The data set collected during Monsoon '90 contains an exceptional variety of measurements from the plant to watershed scale and over a wide range of hydrologic and meteorological conditions experienced in semiarid rangeland environments. These ranged from dry season measurements with dormant vegetation, dry soil moisture, and stable weather conditions to "monsoon" season measurements with actively transpiring vegetation at peak greenness and highly variable water and energy fluxes. During the monsoon field campaign, unstable weather conditions led to several rainfall events occurring with significant spatial gradients in total depth, and to a full range of cloud cover conditions.

A database is being formulated to largely house the data

collected during this experiment, and where necessary, provide both descriptive and professional contact information regarding collection, processing, and reduction of the data. More information regarding this database, as well as phone numbers for dial-in modem access, are contained in Table 2.

The Monsoon '90 research reported in this special section represents an initial attempt to address the specific project research objectives outlined in the introduction. Further research is already under way to fully address the project objectives and to more fully explore, analyze, and model the phenomena observed. Additional efforts will also explore the transferability of the results to other semiarid regions. Under the conditions observed during Monsoon '90, modeling the mass and energy exchanges across the soil-plant-atmosphere interface and through the soil profile is particularly challenging. The results reported here, coupled with the experimental data, should aid the research community in addressing these challenges, provide a firm foundation for future large-scale experimental efforts, and assist in the development and verification of improved methods for quantifying hydrologic and atmospheric fluxes for these environments.

**Acknowledgments.** This project began as a suggestion from a colleague, Ted Engman, now head of the Hydrological Sciences Branch at NASA-GSFC, to write a proposal to NASA in response to an announcement soliciting proposals for interdisciplinary investigations in hydrology. With his help and the guidance of Ray Jackson, Tom Schmutge, Dave Woolhiser, and Larry Hipps, the idea became a reality; and as they say, the rest is history. The cornerstone of this project was the USDA ARS, Walnut Gulch experimental watershed operated by the Southwest Watershed Research Center in Tucson, Arizona, its staff, and on-site personnel who help maintain this unique facility: Howard Larsen, Art Dolphin, Jim Smith, and John Smith in Tombstone, Arizona. The importance of conducting this type of study in a watershed like Walnut Gulch that has a long and detailed hydrologic knowledge base and database cannot be emphasized enough. The participation of many other agencies and institutions which received no direct funding from the project greatly broadened the scope of the study. They include USGS Water Resources Division (Denver and Carson City), USDA ARS Remote Sensing Research Lab and Subtropical Agricultural Research Lab, Los Alamos National Lab, Jet Propulsion Lab, LERTS (France), CEMAGREF-ENGREF (France), IRE (Russia), the University of Arizona (Departments of Hydrology and Water Resources, Soil and Water Science and Optical Sciences, and the School of Renewable Natural Resources), and the University of Maryland (Department of Meteorology). The Landsat 3 MSS image (Plate 1) was produced by the Office of Arid Lands Studies, College of Agriculture, University of Arizona, and a hard copy was provided by Stuart E. Marsh. The Landsat 5 TM used in Plate 1 together with the SPOT 1 HRV 1 satellite image used to produce maps of SAVI for the watershed (Plate 2) was processed by Rob Parry and Karen S. Humes of the USDA ARS Hydrology Lab. The thermal scanner images (Plate 4) were collected and processed by Paul J. Pinter and Lynette Eastman of the USDA ARS U.S. Water Conservation Lab. The NS001 images (Plate 5) were processed by Karen S. Humes with assistance from Rob Parry. A special thanks goes to Rob Parry and Karen S. Humes. Without their assistance, we would not have been able to publish such high-quality remote sensing images for the section. Last, funding from NASA Interdisciplinary Research Program in Earth Sciences (NASA reference number IDP-88-086) and USDA ARS Beltsville Area funds made this study possible, while EOS funding (NAGW2425) provided support for the University of Arizona participants.

## References

- André, J. C., J. P. Goutorbe, and A. Perrier, HAPEX-MOBILHY: A hydrologic atmospheric experiment for the study of water

- budget and evaporation flux at the climatic scale, *Bull. Am. Meteorol. Soc.*, 67, 138-144, 1986.
- Branson, F. A., G. F. Gifford, and R. J. Owen, Rangeland hydrology, Range Sci. Ser., 84 pp., Soc. for Range Manage., Denver, Colo., 1972.
- Chehbouni, A., Y. H. Kerr, J. Qi, A. R. Huete, and S. Sorooshian, Toward the development of a multidirectional vegetation index, *Water Resour. Res.*, this issue.
- Eagleson, P. S., The emergence of global-scale hydrology, *Water Resour. Res.*, 22, 6S-14S, 1986.
- Goodrich, D. C., T. J. Schmugge, T. J. Jackson, C. L. Unkrich, T. O. Keefer, R. Parry, L. B. Bach, and S. A. Amer, Runoff simulation sensitivity to remotely sensed initial soil water content, *Water Resour. Res.*, this issue.
- Hipps, L. E., E. Swiatek, and W. P. Kustas, Interactions between regional surface fluxes and the atmospheric boundary layer over a heterogeneous watershed, *Water Resour. Res.*, this issue.
- Huete, A. R., A soil-adjusted vegetation index (SAVI), *Remote Sens. Environ.*, 25, 295-309, 1988.
- Humes, K. S., W. P. Kustas, M. S. Moran, W. D. Nichols, and M. A. Weltz, Variability of emissivity and surface temperature over a sparsely vegetated surface, *Water Resour. Res.*, this issue (a).
- Humes, K. S., W. P. Kustas, and M. S. Moran, Use of remote sensing and reference site measurements to estimate instantaneous surface energy balance components over a semiarid rangeland watershed, *Water Resour. Res.*, this issue (b).
- Jackson, T. J., et al., Multifrequency passive microwave observations of soil moisture in an arid rangeland environment, *Int. J. Remote Sens.*, 13(3), 573-580, 1992.
- Kustas, W. P., et al., An interdisciplinary field study of the energy and water fluxes in the atmosphere-biosphere system over semiarid rangelands: Description and some preliminary results, *Bull. Am. Meteorol. Soc.*, 72, 1683-1706, 1991.
- Kustas, W. P., M. S. Moran, K. S. Humes, D. I. Stannard, P. J. Pinter, Jr., L. E. Hipps, E. Swiatek, and D. C. Goodrich, Surface energy balance estimates at local and regional scales using optical remote sensing from an aircraft platform and atmospheric data collected over semiarid rangelands, *Water Resour. Res.*, this issue (a).
- Kustas, W. P., J. H. Blanford, D. I. Stannard, C. S. T. Daughtry, W. D. Nichols, and M. A. Weltz, Local energy flux estimates for unstable conditions using variance data in semiarid rangelands, *Water Resour. Res.*, this issue (b).
- Menenti, M., and J. C. Ritchie, Estimation of effective aerodynamic roughness of Walnut Gulch watershed with laser altimeter measurements, *Water Resour. Res.*, this issue.
- Moran, M. S., T. R. Clarke, W. P. Kustas, M. A. Weltz, and S. A. Amer, Evaluation of hydrologic parameters in semiarid rangeland using remotely sensed spectral data, *Water Resour. Res.*, this issue (a).
- Moran, M. S., W. P. Kustas, A. Vidal, D. I. Stannard, J. H. Blanford, and W. D. Nichols, Use of ground-based remotely sensed data for surface energy balance evaluation of a semiarid rangeland, *Water Resour. Res.*, this issue (b).
- National Research Council, *Opportunities in the Hydrologic Sciences*, 348 pp., National Academy Press, Washington, D. C., 1991.
- Perry, E. M., and M. S. Moran, An evaluation of atmospheric corrections of radiometric surface temperatures for a semiarid rangeland watershed, *Water Resour. Res.*, this issue.
- Pinker, R. T., W. P. Kustas, I. Laszlo, M. S. Moran, and A. R. Huete, Basin-scale solar irradiance estimates in semiarid regions using GOES 7, *Water Resour. Res.*, this issue.
- Qi, J., A. R. Huete, F. Cabot, and A. Chehbouni, Bidirectional properties and utilizations of high-resolution spectra from a semiarid watershed, *Water Resour. Res.*, this issue.
- Renard, K. G., The hydrology of semiarid rangeland watersheds, *Publ. 41-162, Agric. Res. Serv., U.S. Dep. of Agric.*, Washington, D. C., 1970.
- Renard, K. G., L. J. Lane, J. R. Simanton, W. E. Emmerich, J. J. Stone, M. A. Weltz, D. C. Goodrich, and D. S. Yakowitz, Agricultural impacts in an arid environment: Walnut Gulch case study, *Hydrol. Sci. Technol.*, 9(1-4), 145-190, 1993.
- Schlesinger, W. H., J. F. Reynolds, G. L. Cunningham, L. F. Huenneke, W. M. Jarvell, R. A. Virginia, and W. G. Whitford, Biological feedbacks in global desertification, *Science*, 24, 1043-1048, 1990.
- Schmugge, T. J., T. J. Jackson, W. P. Kustas, R. Roberts, R. Parry, D. C. Goodrich, S. A. Amer, and M. A. Weltz, Push broom microwave radiometer observations of surface soil moisture in Monsoon '90, *Water Resour. Res.*, this issue.
- Segal, M., W. E. Schreiber, G. Kallos, J. R. Garratt, A. Rodi, J. Weaver, and R. A. Pielke, The impact of crop areas in northeast Colorado on mid summer mesoscale thermal circulations, *Mon. Weather Rev.*, 117, 809-825, 1989.
- Sellers, P. J., F. G. Hall, G. Asrar, D. E. Strebel, and R. E. Murphy, The first ISLSCP field experiment (FIFE), *Bull. Am. Meteorol. Soc.*, 69, 22-27, 1988.
- Stannard, D. I., J. H. Blanford, W. P. Kustas, W. D. Nichols, S. A. Amer, T. J. Schmugge, and M. A. Weltz, Interpretation of surface flux measurements in heterogeneous terrain during the Monsoon '90 experiment, *Water Resour. Res.*, this issue.
- Stidd, C. K., Irrigation increases rainfall?, *Science*, 188, 279-280, 1975.
- van de Griend, A. A., M. Owe, H. F. Vugts, and S. D. Prince, Water and surface energy balance modeling in Botswana, *Bull. Am. Meteorol. Soc.*, 70, 1404-1411, 1989.
- Weltz, M. A., J. C. Ritchie, and H. D. Fox, Comparison of laser and field measurements of vegetation height and canopy cover, *Water Resour. Res.*, this issue.

D. C. Goodrich, USDA Agricultural Research Service, Southwest Watershed Research Center, 2000 East Allen Road, Tucson, AZ 85719.

W. P. Kustas, USDA Agricultural Research Service, Hydrology Laboratory, Building 007, Room 140 BARC West, Beltsville, MD 20705.

(Received October 5, 1992; revised October 15, 1993; accepted October 19, 1993.)